Au-Core/Pt-Shell Bimetallic Cluster-Loaded TiO_2. 1. Adsorption of Organosulfur Compound

Hiroaki Tada,*,† Fumiaki Suzuki,‡ Seishiro Ito,‡ Tomoki Akita,§ Koji Tanaka,§ Tetsuro Kawahara,|| and Hisayoshi Kobayashi⊥

Molecular Engineering Institute, Kinki University, 3-4-1, Kowakae, Higashi-Osaka, Osaka 577-8502, Japan, Department of Applied Chemistry, Faculty of Science and Engineering, Kinki University, 3-4-1, Kowakae, Higashi-Osaka, Osaka 577-8502, Japan, National Institute of Advanced Industrial Science and Technology, Midorigaoka 1-8-31, Ikeda, Osaka 563-8577, Japan, Nippon Sheet Glass Co. Ltd., 1-7, 2-Chome, Kaigan, Minato-Ku, Tokyo 105-8552, Japan, and Department of Chemical Technology, Kurashiki University of Science and Arts, 2640 Nishinoura, Tsurajima, Kurashiki 712, Japan

Received: January 29, 2002; In Final Form: June 2, 2002

Au-core/Pt-shell bimetallic clusters have been loaded on the surface of TiO_2 (Au(x wt %)−Pt(y wt %)−TiO_2(Pt/Au atomic ratio, z)) in a highly dispersed state by a two-step method consisting of the Au deposition and the subsequent Pt photodeposition. The mean diameter of the metal particles increases as a result of the Pt deposition from 3.6 ($x = 0.39$, $y = 0$, $z = 0$) to 4.3 nm ($x = 0.37$, $y = 0.74$, $z = 2.0$), while their number density hardly changes. High-resolution transmission electron spectroscopy directly confirms an Au-core/Pt-shell structure for a sample ($z = 0.82$). Adsorption experiments of bis(2-dipyridyl) disulfide, selected as a sulfur-containing compound, clarify that it adsorbs preferentially on the metal surfaces and the saturated adsorption amount on Au−Pt/TiO_2 significantly decreases as compared to those on Au/TiO_2 and Pt/TiO_2. From X-ray photoelectron spectroscopic measurements, the $Pt^4{}_{f_{7/2}}$ binding energy for the Au−Pt/TiO_2 sample has been found to shift to a lower energy relative to that for bulk Pt by 1.4 eV. Also, the Pt photodeposition causes a red shift in the absorption maximum of the Au plasmon band. These spectroscopic results are rationalized in terms of the partial electron transfer from Au to Pt, which is also suggested by the calculations of a model cluster (Au_2−Pt_2/TiO_2) using the density functional theory (DFT). Further, the DFT calculations indicate that the bonding and antibonding metal−sulfur orbitals are formed and the latter contribution is more significant to the bond for the Pt-containing clusters.

1. Introduction

In heterogeneous photocatalysis, oxidation and reduction proceed simultaneously at adjacent sites on the surface of photocatalyst. This essentially causes the decrease in the reaction efficiency, while unique products are sometimes obtained.[1] Loading of nanometer-sized noble[2] or coinage metals[3−5] onto the surface of TiO_2, a representative semiconductor photocatalyst, generally enhances the charge separation efficiency and/or the adsorptivity for substrates to increase its activity.[2] On the other hand, bimetallic catalysts are known to exhibit the synergies including "ensemble effect" and "ligand effect".[6−8] The former results from geometrical arrangement of surface atoms in a fashion appropriate for a particular reaction to occur. The latter is induced by modification of the electronic state(s) of either or both host and guest metals. Thus, bimetallic cluster-loaded TiO_2 (M_1−M_2/TiO_2) has a potential to achieve high activity and selectivity in photocatalysis through fine-tuning of the topology and/or the electronic state of surface atoms. However, there have been only a few studies on the photocatalysis of bimetallic cluster-loaded TiO_2.[9,10] We have recently found that hydrogen is generated from water by cycling dark adsorption and successive photoinduced desorption of 2-mercaptopyridine (RSH) on/from Ag-core/Pt-shell cluster loaded on TiO_2.[10] In photocatalysis, the interfacial electron transfer in M_1−M_2/TiO_2 is of great interest in two points. The charge transfer from M_1 to M_2 (or vice versa) *in the dark* can affect the adsorption property for substrates. Also, the photocatalytic activity of TiO_2 can depend on the electron transfer from TiO_2 to the substrate via M_1 and M_2 *in the photostationary state*. Particularly, in the core−shell type bimetal, since the charge transfer is one-directional (vectorial), these effects would be enhanced.

Au-core/Pt-shell bimetallic cluster-loaded TiO_2 particles (Au_c−Pt_s/TiO_2) were prepared by a two-step method consisting of the first process for depositing Au clusters[11] and the second process for depositing Pt photocatalytically. This paper describes the characterization results of Au−Pt/TiO_2, with an emphasis placed on the electronic state. Also, the adsorptivity of the metal clusters for a sulfur-containing compound (SCC), bis(2-dipyridyl) disulfide (RSSR), was examined. Further, theoretical calculations using the density functional theory (DFT) were performed in order to obtain the deep understanding of the bonding between the metal clusters and the SCC.

* Author to whom correspondence should be addressed: Tel: +81-6-721-2332. Fax: +81-6-721-3384. E-mail: h-tada@apsrv.apch.kindai.ac.jp.
† Molecular Engineering Institute, Kinki University.
‡ Department of Applied Chemistry, Faculty of Science and Engineering, Kinki University.
§ National Institute of Advanced Industrial Science and Technology.
|| Nippon Sheet Glass Co. Ltd.
⊥ Kurashiki University of Science and Arts.

10.1021/jp0202690 CCC: $22.00
Published on Web 08/01/2002

2. Experimental Section

Anatase TiO_2 particles were supplied from Ishihara Techno Co. (A100) and used without further activation. The specific surface area was determined to be 8.1 $m^2\ g^{-1}$ from N_2 gas adsorption at −196 °C based on the BET equation. Water was used after being passed through an ion-exchange resin. A KI−I_2 aqueous solution was added dropwise to a solution of 2-mercaptopyridine (40.4 g, 360 mmol, >95%, Tokyo Kasei) in a 2 M NaOH aqueous solution (500 mL) until the reaction mixture turned brown. To this solution, an aqueous solution of $Na_2S_2O_3$ was added, and then extracted with benzene (200 mL) three times. The benzene layer was washed with water and dried over $MgSO_4$. After the solvent had been evaporated, the residue was purified by recrystallization from a mixed solvent of *n*-hexane and benzene to yield RSSR: yield, 72%; mp, 57−58 °C; ^{1}H NMR (60 MHz, $CDCl_3$, δ ppm); 7.03−7.50 (m, 3Py, 3′Py, 5Py, 5′Py 4H), 8.57 (d, 4Py, 4′Py, 2H), 8.60 (d, 6Py, 6′Py, 2H). Other reagents used in this work had at least a level of GR and were used without further purification. Nanometer-sized Au particles were deposited on the surface of TiO_2 by the deposition−precipitation method.[11] After the pH of a 4.86×10^{-3} M aqueous solution (100 mL) of $HAuCl_4 \cdot 4H_2O$ (Kishida Chemicals, >99.3%) had been adjusted to 6.0 with a 0.4 M NaOH, TiO_2 particles (10 g) were suspended and aged with stirring at 70 °C for 1 h. The particles were washed with distilled water three times and kept under vacuum at room temperature. The dried particles were calcined at 400 °C for 4 h in air in an electric oven. The TiO_2 or Au/TiO_2 particles (5 g) were suspended in 200 mL of an ethanol solution of platinum acetylacetonate ($Pt(acac)_2$, Soekawa Chemicals, >99%). After the suspension had been stirred for 24 h in the dark, irradiation ($\lambda_{ex} > 300$ nm) was carried out with a 400-W high-pressure mercury arc (H-400P, Toshiba) under an N_2 atmosphere. The light intensity integrated from 320 to 400 nm ($I_{320-400}$) was measured to be 4.3 mW cm^{-2} using a digital radiometer (DRC-100X, Spectroline). The suspension was magnetically stirred during the irradiation. The resultant sample was washed by repeating washing/centrifugation (1.3×10^4 rpm, 2 min) three times and dried in a vacuum desiccator at room temperature. The metal deposits on TiO_2 were dissolved by treating the particles (1 g) with aqua regia (50 mL). The concentrations of Au^{3+} and Pt^{4+} ions in the resultant solutions were determined by induced coupled plasma spectroscopy (ICPS-1000, Shimadzu). The catalysts loaded with *x* wt % of Au and *y* wt % of Pt was denoted as Au(*x* wt %)−Pt(*y* wt %)/TiO_2(*z*); *z* is the atomic ratio of Pt to Au. The size and distribution of metal particles deposited on TiO_2 were observed by a transmission electron microscope (JEOL, JEM-3010) at an acceleration voltage of 300 kV. High-resolution transmission electron microscopic (HRTEM) measurements were carried out using a JEOL JEM-3000F (applied voltage = 300 kV). The energy-dispersive X-ray spectra (EDS) were obtained at a beam radius below 3 nm during 100 s with a takeoff angle of 20° and a solid angle of 0.09 (steradian). X-ray photoelectron spectroscopic (XPS) measurements were performed using a PHI 5600Ci spectrometer with an mono-chromated Al Kα X-ray source operated at 14 kV and 150 W. The takeoff angle was 45° and typical operating pressures were 1×10^{-8} Pa. Multiplex (narrow-scan) spectra were obtained for Ti_{2p}, Au_{4f}, and Pt_{4f} photopeaks. The line shapes used for curve fitting were Gaussian, and the integrated backgrounds were employed. All the binding energies were referenced with respect to the carbon peak of C−H at 285.0 eV. Electronic absorption spectra of RSSR were recorded in the 200−500 nm range on an ultraviolet−visible spectrophotometer (U-4000, Hitachi), and its absorptivity at 281 nm was determined to be $\epsilon_{max} = 1.05 \times 10^4\ M^{-1}\ cm^{-1}$. Adsorption isotherms of RSSR at 25 ± 1 °C were obtained by equilibrating the catalysts to the solutions with varying concentrations in the dark followed by centrifugation and spectrophotometric analysis of RSSR remaining in the solutions.

3. DFT Calculation Method

The TiO_2 surface is modeled by a $Ti_4O_{10}H_4$ cluster, which is truncated from the rutile (110) surface. The hydrogen atoms are used to stabilize the dangling bond at the peripheral O atoms. To minimize the artificial effects by such H atoms, we impose a criterion that the metal oxide clusters should be stoichiometric composition and an integer number of water molecules is added. The $Ti_4O_{10}H_4$ cluster is decomposed to Ti_4O_8 and $2H_4O$, and satisfies the criterion. Metal particles are modeled by tetrahedral shaped Ag_4, Au_4, Pt_4, and Au_2Pt_2 clusters. The tetrahedral structure does not correspond to the most stable one for a free cluster, but it is stable on the $Ti_4O_{10}H_4$ cluster. Figure 5A shows the optimized structure of $Au_2-Pt_2/Ti_4O_{10}H_4$ as the representative of $M_4/Ti_4O_{10}H_4$ (M = Ag, Au, or Pt). In this type of calculations, the M atoms and one O atom, which is at the upper position and closest to M atom, are optimized, and the other part of $Ti_4O_{10}H_4$ cluster is fixed to the crystalline geometry. (The O−H bond length is fixed to 1.0 Å) In case of adsorption of RS, the RS moiety is optimized as well as the metal part and one O atom. The Gaussian 98 program is used in this work.[12] The gradient-corrected DFT is employed in this calculation.[13] The used functionals are the Hartree−Fock, Slater[14] and Becke exchange,[15] and the Lee−Yang−Parr[16] and Vosko−Wilk−Nusair[17] correlation functionals (B3LYP). For Ti, Ag, Au, and Pt atoms, the Los Alamos model core potentials (MCP)[18] and corresponding basis sets[19] are used as implemented in the program.

4. Results and Discussion

Formation of Au_c-Pt_s Bimetallic Clusters on TiO_2 Surfaces. Figure 1 shows TEM photographs of the metal-loaded TiO_2 particles: A, Au/TiO_2; B, $Au-Pt/TiO_2$. In Figure 1A, many Au particles with a diameter of ca. 3 nm are fixed on the TiO_2 surfaces in a highly dispersed state. In Figure 1B, the mean size of the metal particle increases with the Pt photodeposition, whereas it is apparent that the number density hardly changes. This suggests that Pt deposits mainly on the Au surfaces of Au/TiO_2. Figure 2A is an HRTEM photograph of the $Au-Pt/TiO_2$ particles, directly demonstrating that the metal cluster has a core−shell structure. Irradiation with an electron beam focused on the single metal particle indicated with an arrow in Figure 2A yielded the EDS shown in Figure 2B. The particle consists of Au and Pt, which was also true for most other particles, and no independent Pt particle could be detected by the EDS measurements. The signals of Cu arise from a copper mesh used for fixation of the particles. It is reasonable to conclude that the photodeposition of Pt occurs selectively on the Au surfaces of Au/TiO_2 ($Au(TiO_2)$), leading to the formation of a Au-core/Pt-shell bimetallic structure on TiO_2. Figure 3 shows the size distribution of the bimetallic clusters loaded on TiO_2 with the following compositions; A($x = 0.39$, $y = 0$, $z = 0$), B(0.34, 0.15, 0.45), and C (0.37, 0.27, 0.74). The mean diameter (*d*), indicated by the arrow, increases with an increase in the amount of Pt deposited.

The mechanism of the Pt photodeposition on Au/TiO_2 can be presumed as follows. Upon excitation of Au/TiO_2 (eq 1), a portion of the electrons in the conduction band (cb) of TiO_2

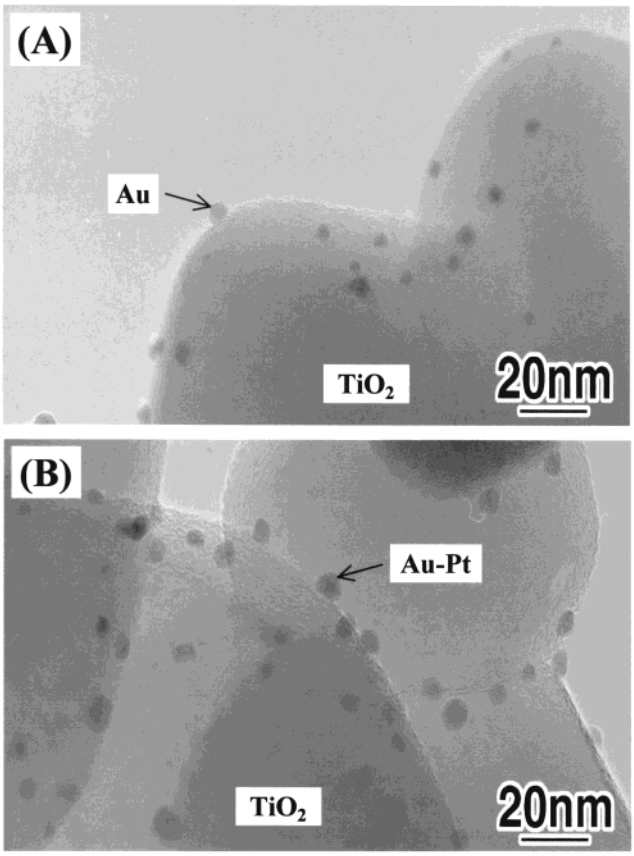

Figure 1. TEM photographs of metal-loaded TiO_2 particles: (A) Au/TiO_2; (B) Pt−Au/TiO_2 ($z = 0.44$).

flow into Au with a large work function (eq 3). This process is effective in decreasing the probability of recombination of the electron−hole pairs (eq 2).[20] Consequently, the Au particles act as reduction sites, while C_2H_5OH is oxidized on the TiO_2 surfaces (eq 4). Additional electrons arise from continuing band-gap excitation of TiO_2 (Au($2e^-$)/TiO_2 in eq 5). Also, the C_2H_4-OH radical can inject another electron into the cb of TiO_2.[21] Therefore, Pt is thought to deposit selectively on the Au(TiO_2) surfaces (eq 5).

$$Au/TiO_2 + h\nu \rightarrow Au/TiO_2(e^- \cdots h^+) \quad (1)$$

$$Au/TiO_2(e^- \cdots h^+) \rightarrow Au/TiO_2 \quad (2)$$

$$Au/TiO_2(e^- \cdots h^+) \rightarrow Au(e^-)/TiO_2(h^+) \quad (3)$$

$$Au(e^-)/TiO_2(h^+) + C_2H_5OH \rightarrow H^+ + C_2H_4OH + Au(e^-)/TiO_2 \quad (4)$$

$$Au(2e^-)/TiO_2 + Pt^{2+} \rightarrow Au\text{-}Pt/TiO_2 \quad (5)$$

This selective photodeposition of Pt on Au(TiO_2) suggests an electrically good contact between Au and TiO_2. The efficient electron flow from the cb of TiO_2 to Pt through Au in the photostationary state is an important requirement of the photocatalytic reaction of Au−Pt/TiO_2.

Characterization of the Metal Nanoparticles. Figure 4 shows the Ti_{2p} (A), Au_{4f} (B), and Pt_{4f} (C) XPS spectra of the samples: #1, Pt(0.20)/TiO_2; #2, Au(0.39)/TiO_2; #3, Au(0.38)−Pt(0.053)/TiO_2(0.14). The comparison of spectra A and B indicates that the intensity ratio of the $Au^4{}_{f_{7/2}}$ signal to the $Ti^2{}_{p_{3/2}}$

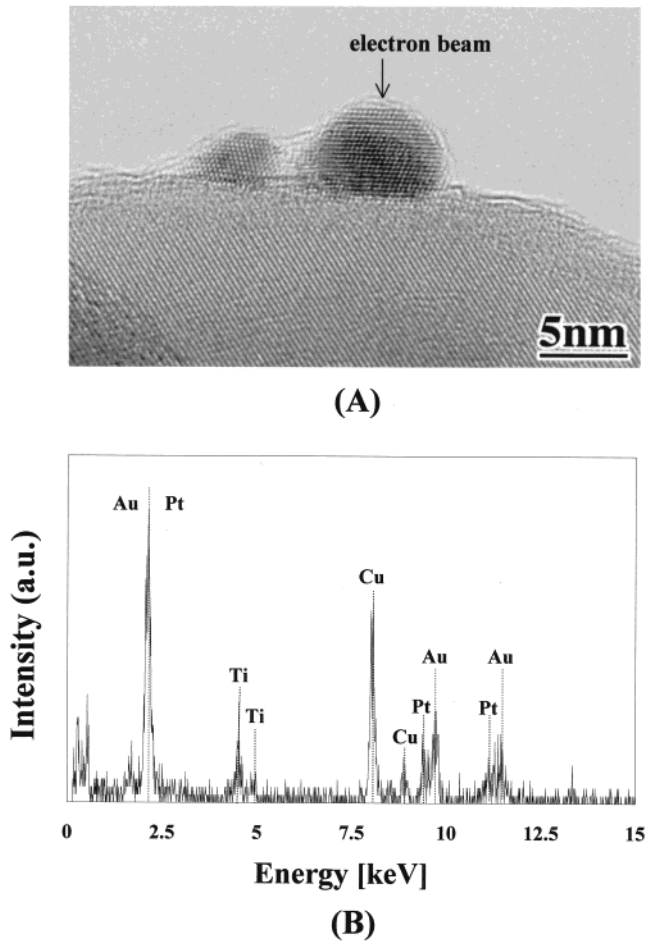

Figure 2. HRTEM photograph of the Au−Pt/TiO_2 particles (A) $z = 0.82$, and the EDS of the arrowed single metal particle in Figure 2A (B).

signal for #3 is much smaller than that for #2. This finding supports the idea induced by the TEM observation that most Au particles are covered with Pt in #3.

In spectrum C, the $Pt^4{}_{f_{7/2}}$ binding energy (E_B) decreases in the order of Pt foil (standard) > #1 > #3. Table 1 lists the detailed numerical XPS data. Fung and Tanaka et al. found that the E_B of the Pt nanoparticles deposited on TiO_2 by vacuum evaporation shifts to a higher energy by ca. 1.5 eV with relative to that of a bulk Pt sample.[22,23] This was attributed to the decrease in the polarization energy with decreasing size of the Pt particle. In contrast, the E_B of #1 shifts to a lower energy by 0.8 eV with relative to the reference. The specific strong interaction between Pt and TiO_2, which appears on heating Pt/TiO_2 under H_2 at about 773 K, is known as "strong metal−support interaction (SMSI)".[24] The SMSI state of Pt/TiO_2 is characterized by the two facts: one is the very low E_B's ranging from 70.7 to 71.1 eV and the other is that neither H_2 nor CO adsorbs on the surface. The E_B of #1 is close to that of the sample in a SMSI state; however, CO and H_2 adsorption experiments previously confirmed that Pt/TiO_2 prepared by photodeposition does not exhibit the SMSI state.[25] The mechanism on appearance of the SMSI state is considered as involving the electron transfer from Ti^{3+} ions to Pt via oxygen vacancy.[26] As stated above, since the photodeposition of Pt on TiO_2 is an electrochemical process, the resultant Pt/TiO_2 is natively endowed with the electrically good contact between Pt and TiO_2. The electron transfer from TiO_2 to Pt due to the difference in Fermi energy seems to explain the chemical shift from 71.2 to 70.4 eV. Brus reported that the Fermi energy for

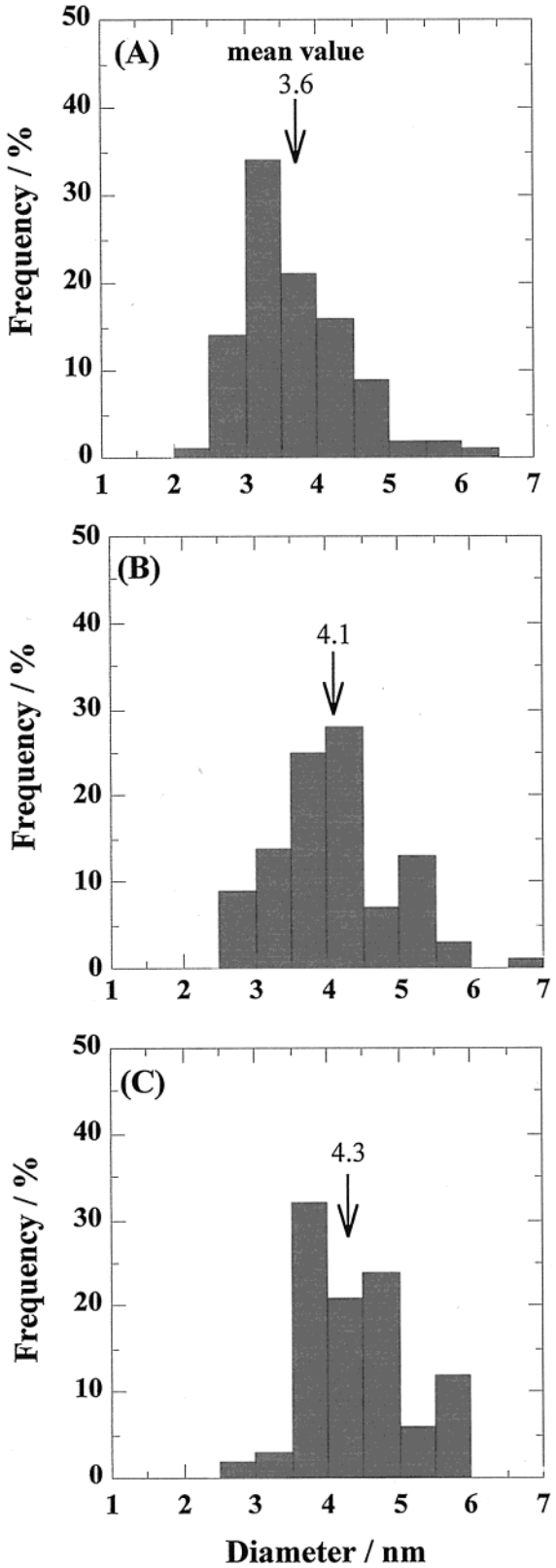

Figure 3. Size distribution of the bimetallic particles loaded on TiO_2; (A) ($x = 0.39$, $y = 0$, $z = 0$); (B) (0.34, 0.15, 0.45); (C) (0.37, 0.27, 0.74). The arrow indicates the mean diameter.

intrinsic TiO_2 to be 5.5 eV,[27] which is smaller than that of Pt (5.65 ± 0.1 eV).[28] The low-temperature process, in which oxygen vacancy is difficult to yield on the surface of TiO_2, may be responsible for the non-SMSI state.

The E_B of #3 is further smaller than that of #1 by 0.6 eV, indicating that the Pt is in a very electron-rich state. Electronic

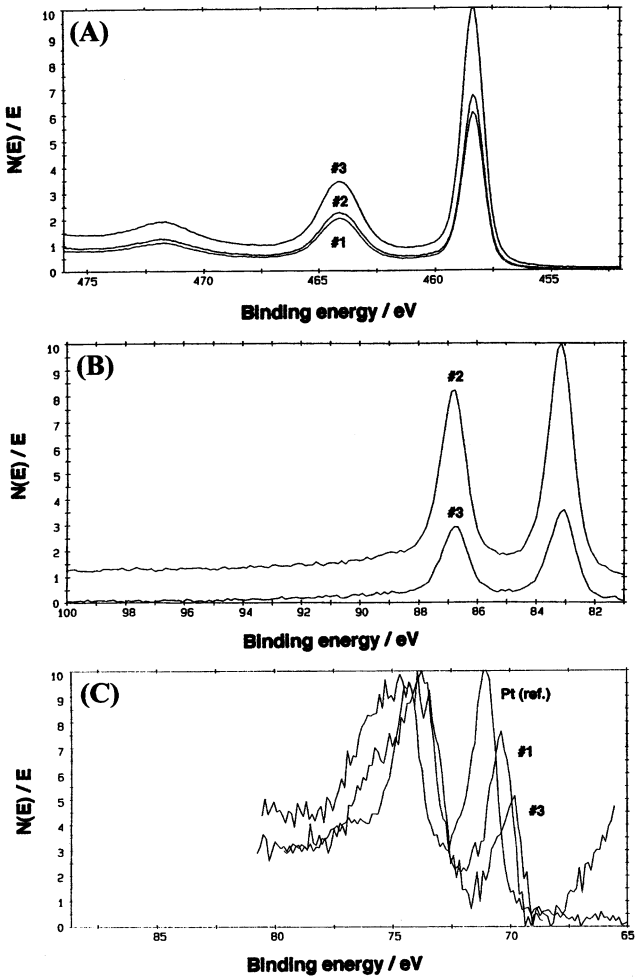

Figure 4. Ti_{2p} (A), Au_{4f} (B), and Pt_{4f} (C) XPS spectra of the samples: #1, Pt/TiO_2; #2, Au/TiO_2; #3, $Au(0.37)-Pt(0.053)/TiO_2(0.14)$.

TABLE 1: Results of XPS Analyses of Pt/TiO_2 and on $Au-Pt/TiO_2$

samples	state	E_B ($^4f_{7/2}$)/eV	fwhm ($^4f_{7/2}$)/eV
Au	Au^0	83.1	
Pt-foil	Pt^0	71.2 (71.0[a])	1.3
Pt/TiO_2	$Pt^{\delta-}$	70.4 (71.1[a]/70.7[b])	1.3 (1.6[b])
$Au-Pt/TiO_2$	$Pt^{\delta-}$	69.8	1.4

[a] Data showing the values reported by Fung for the Pt/TiO_2 sample prepared by vacuum deposition and subsequent heating at 623 K under H_2.[22] [b] Data cited from the work by Tanaka et. al., in which the sample was heavily reduced by Ar-ion bombardment.[23] Also, its SMSI state was confirmed by CO-adsorption experiments at 77 K.

absorption spectra (AS) were measured for the $Au-Pt/TiO_2(0 \le z \le 0.30)$ particles. At $z = 0$, an absorption band due to the plasmon of Au nanoparticles is situated at 539 nm. The deposition of Pt on $Au(TiO_2)$ gives rise to a slight red shift of the band simultaneously with its broadening ($0.017 \le z \le 0.30$). Also, as the value of z increases, the red shift is more pronounced at $z < 0.16$. The plasmon absorption band is known to be quite sensitive to changes in the electronic structure of nanoparticles. The red shift of the band is attributable to the decrease in the electron density of Au with the postdeposition of Pt.[29] These results of XPS and AS provide evidence for the interfacial electron transfer from $Au(TiO_2)$ to Pt.

The optimized structure of $Au_2-Pt_2/Ti_4O_{10}H_4$ is shown in Figure 5A. In the calculations, the C_s symmetry is imposed. Similar structures of $M_4/Ti_4O_{10}H_4$ clusters were obtained for the four metals (M = Ag, Au, Pt, and Au−Pt), and the

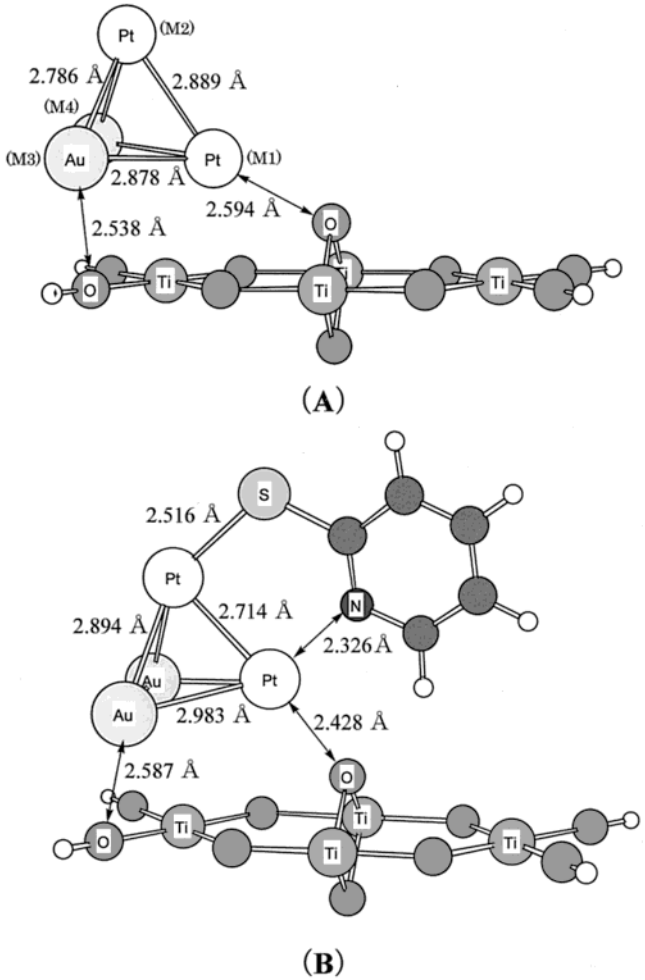

Figure 5. The optimized structures of $Au_2-Pt_2/Ti_4O_{10}H_4$ (A) and RS/$Au_2-Pt_2/Ti_4O_{10}H_4$ (B).

TABLE 2: Typical Geometrical Parameters for $M_4/Ti_4O_{10}H_4$ and RS/$M_4/Ti_4O_{10}H_4$ Systems[a]

cluster	M1−M2	M1−M3	M2−M3	M1−O	M3−O	M1−N	M2−S
Ag_4	2.926	2.936	3.291	2.385	2.452		
Au_4	2.754	2.972	3.165	2.427	2.539		
Pt_4	2.861	2.838	2.903	2.914	2.403		
Au_2-Pt_2	2.889	2.878	2.786	2.594	2.583		
RS/Ag_4	2.867	3.164	2.997	2.552	2.504	2.362	2.365
RS/Au_4	2.839	2.997	2.911	2.545	2.516	2.413	2.605
RS/Pt_4	2.761	2.969	2.768	2.355	2.362	2.287	2.460
RS/Au_2-Pt_2	2.714	2.983	2.894	2.428	2.587	2.326	2.516

[a] Unit is angstrom.

TABLE 3: Atomic Charges on Metal Atoms For $M_4/Ti_4O_{10}H_4$ Clusters

	population					
	Mulliken population			natural population		
cluster	M1	M2	M3	M1	M2	M3
Ag_4	0.280	0.039	0.098	0.394	−0.172	0.554
Au_4	0.233	−0.084	−0.008	0.345	−0.169	0.441
P_{t4}	−0.011	−0.011	0.004	0.213	−0.017	0.101
Au_2-Pt_2	−0.052	−0.034	0.026	0.067	−0.284	0.376

tetrahedral structures were stable on the $Ti_4O_{10}H_4$ support; Table 2 summarizes the geometrical parameters. Table 3 shows the charge on metal atoms estimated by the Mulliken and natural population analysis of the $M_4/Ti_4O_{10}H_4$ model clusters. Both populations indicate similar trends, and the natural population analysis is clearer. For the pure metal clusters, M1 and M3 atoms

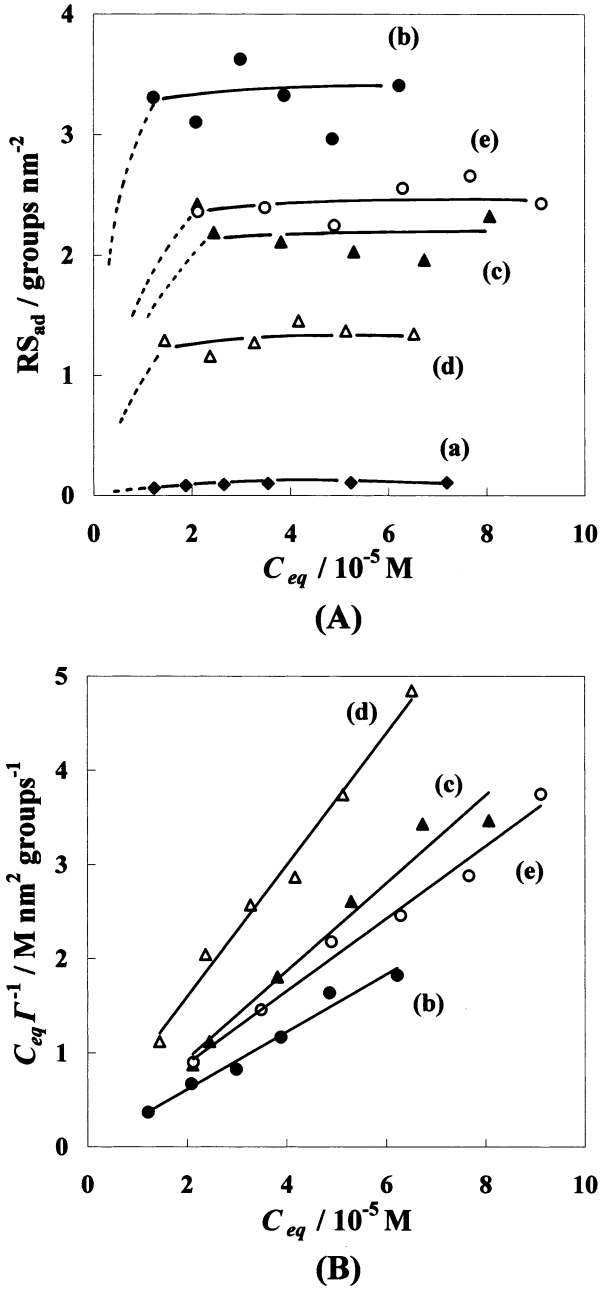

Figure 6. (A) Adsorption isotherms of RSSR on the various particles at 25 ± 1 °C: a, TiO_2; b, Au(0.39)/TiO_2; c, Pt(0.20)/TiO_2; d, Au(0.41)−Pt(0.025)/TiO_2(0.062); e, Au(0.37)−Pt(0.28)/TiO_2(0.76). (B) The Langmuir plots for the metal/TiO_2 systems: C_{eq} and Γ are the equilibrium concentration of RSSR and the adsorption amount, respectively.

have large positive charges due to the interaction with O atoms, and the M2 atom, which is distant from the O atoms, has a negative charge. For Pt_4, the polarization is small, and the whole charge summed over the four metal atoms is much less positive compared to Ag_4 and Au_4. On the other hand, for Au_2-Pt_2, the Pt atoms (designated by M1 and M2) become more negative than the Au atoms (designated by M3), and the electronic polarization is larger again. The polarity of polarization ($Au^{\delta+}-Pt^{\delta-}$) is opposite to that expected from the electronegativity scale (χ(Pt) = 2.28, χ(Au) = 2.54).[30] This theoretical result on the metal cluster also corresponds well to the partial electron transfer from Au(TiO_2) to Pt in Au−Pt/TiO_2.

Adsorption of RSSR on the Metal Nanoparticle Surfaces. Figure 6A shows the adsorption isotherms of RSSR on various

TABLE 4: Γ_s and ΔE Values for the Metal Clusters Loaded on TiO_2

metal	Γ_S/groups nm^{-2}	ΔE/kcal mol^{-1}
Ag(111)	3.6[a]	73
Au(TiO_2)	3.1 ± 0.1	64
Pt(TiO_2)	2.3 ± 0.3	59
Au−Pt(TiO_2)	1.46	35

[a] This is the datum determined for the Ag(111) surface.[34]

particles at 25 ± 1 °C: a, TiO_2; b, Au(0.39)/TiO_2; c, Pt(0.20)/TiO_2; d, Au(0.41)−Pt(0.025)/TiO_2(0.062); e, Au(0.37)−Pt(0.28)/TiO_2(0.76). Previous studies using high-resolution electron energy loss[31] and Raman scattering[32] spectroscopies revealed that RSSR adsorbs on both Au and Pt surfaces accompanied by cleavage of the S−S bond. The mole numbers of the RS group adsorbed per unit surface area of the metal particles were calculated from the adsorption amount of RSSR, and the mean diameter and loading quantity of the metals. It was assumed that all the metal particles are hemispherical and that the density of RSSR adsorbed on the naked TiO_2 surfaces is invariant with metal deposition. This figure indicates that RSSR adsorbs preferentially on the metal surfaces. Figure 6B shows the Langmuir plots for the metal(TiO_2) systems: C_{eq} and Γ are the equilibrium concentration of RSSR and its adsorption amount, respectively. The good linearity in each plot suggests that the RS groups form a monolayer on the metal surfaces; this is well-known in the Au and Ag electrode systems as "self-assembled monolayers".[33] The saturated adsorption amount of the RS group (Γ_s/groups nm^{-2}) for TiO_2, Au(TiO_2), Pt(TiO_2), and Au−Pt(TiO_2) ($z = 0.16$) were calculated to be 0.13, 3.1 ± 0.1, 2.3 ± 0.3, and 1.46 groups nm^{-2}, respectively. The Γ_s values for Au(TiO_2) and Pt(TiO_2) were comparable to that of RSH in a close-packed adsorption state on the Ag(111) surface determined by Auger spectroscopy (3.6 groups nm^{-2}).[34] The formation of such close-packed monolayers is mainly due to the strong metal−S bond (vide infra). Noticeably, the Γ_s value for Au−Pt(TiO_2) is significantly smaller than those for Au(TiO_2) and Pt(TiO_2), i.e., the adsorptivity for RSSR weakens as a result of the Pt photodeposition.

As a model for the Au−Pt cluster loaded on TiO_2, the mixed metal atom cluster Au_2−Pt_2/$Ti_4O_{10}H_4$ is employed. The optimized structure of RS/Au_2−Pt_2/$Ti_4O_{10}H_4$ is shown in Figure 5B, and its optimized geometrical parameters are also shown in Table 2. Upon adsorption of the RS group, the S and also N atoms interact with metal atoms. The adsorption energies of RS ($\Delta E = E$(RS/M_4/$Ti_4O_{10}H_4$) − E(M_4/$Ti_4O_{10}H_4$) − $^1/_2E$(RSSR)) calculated for Ag_4, Au_4, Pt_4, and Au_2−Pt_2 are 73, 64, 59, and 35 kcal mol^{-1}, respectively. As shown in Table 4, the order of ΔE, $Ag_4 > Au_4 > Pt_4 > Au_2$−$Pt_2$ is in agreement with that of the Γ_s value, Γ_s(Ag(111)) > Γ_s(Au(TiO_2)) > Γ_s(Pt(TiO_2)) > Γ_s(Au−Pt(TiO_2) with $z = 0.16$). The coverage of Au with Pt (θ) can be estimated by the atomic ratio of Pt atoms/surface Au atoms.[35] The z value of 0.16 corresponds to the θ of 0.64. The DFT calculation correctly predicts the relative adsorptivity of the metal clusters loaded on TiO_2 for RSSR. It should also be noted in Figure 6 that the adsorptivity depends on z (or θ), i.e., the coverage of Au with Pt significantly lowers the adsorptivity at $z = 0.062$ ($\theta = 0.25$), while it is comparable to that of Pt/TiO_2 at $z = 0.76$ ($\theta = 3.0$). This implies that a unique surface electronic state, induced by the electron transfer from Au to Pt at $\theta < 1$, approaches that of bulk Pt at $\theta > 1$.

Surface Bonding of the Organosulfur Compound to the Metal Clusters(TiO_2). Figure 7 shows the variations of the λ_{max} of the Au plasmon band before (a, c) and after (b, d) the RSSR adsorption on the metal/TiO_2 particles: (a, b) and (c, d) are the spectra for the samples with the metals ($x = 0.39$, $y = 0$, $z = 0$) and (0.38, 0.21, 0.56), respectively. In each case, the λ_{max} slightly increases as a result of the RSSR adsorption, and the amount of the red shift is greater for the sample without Pt. This finding suggests that electron transfer occurs from Au to the adsorbed RS group through Pt. Jennings and Labinis confirmed by XPS spectroscopy that the bonds between thiols (or disulfides) and coinage metals have a large ionic character ($RS^{\delta-}$−$metal^{\delta+}$).[36]

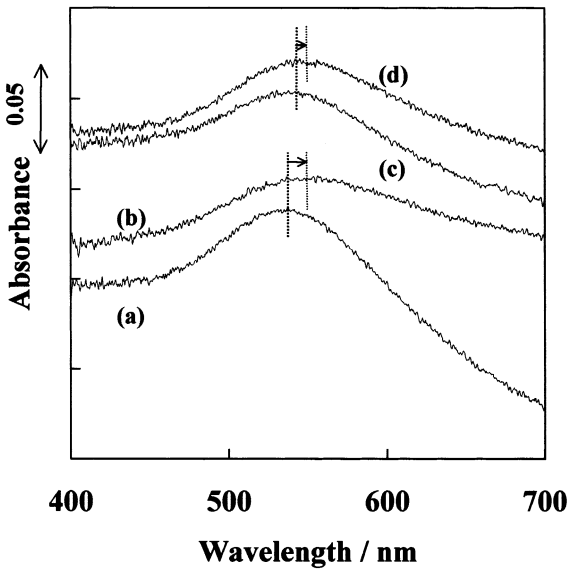

Figure 7. Electronic absorption spectra of the Au−Pt/TiO_2 particles before (a, c) and after (b, d) adsorption of RSSR: a and b are the data for the sample(0.39, 0, 0); c and d are the data for the sample(0.38, 0.21, 0.56).

The Mulliken bond population indicates the strength of the metal−sulfur bond. The sulfur atom interacts with a single metal atom (Figure 5B), and the corresponding bond population values for Au_4, Pt_4, and Au_2−Pt_2 metals are 0.294, 0.236, and 0.201, respectively, in the RS/M_4/$Ti_4O_{10}H_4$. The good correspondence of ΔE and the bond population suggests that the metal−S bond plays a definitive role in the interaction between the metal cluster and the RS group. The orbital contour maps (data not shown) revealed that the metal−sulfur antibonding character is weak for the Au_4 cluster, but stronger for the Pt_4 and Au_2−Pt_2 clusters. The HOMO energy shifts to downward in the order of Ag_4, Au_4, Pt_4, and Au_2−Pt_2. The energy for Au_2−Pt_2/$Ti_4O_{10}H_4$ (−5.99 eV) is close to that for the RS$^\bullet$ radical (−6.32 eV), and the HOMO−HOMO antibonding interaction becomes strong in the same order. From these results, the conclusion can be drawn that the HOMO−HOMO antibonding interaction is the important factor to control the strength of the bonding between the metal(TiO_2) and the SCCs.

5. Conclusions

The selective photodeposition of Pt onto Au(TiO_2) particles prepared by the deposition−precipitation method led to the formation of Au(core)−Pt(shell) bimetallic cluster-loaded TiO_2 particles (Au−Pt/TiO_2). The very low $Pt^4{}_{f_{7/2}}$ E_B of Au−Pt/TiO_2 and the red shift in the λ_{max} indicated that the partial electron transfer from Au to Pt. The electronic polarization ($Au^{\delta+}$−$Pt^{\delta-}$), whose direction is opposite to that expected from the usual electronegativity scale, is supported by the DFT calculations for a model cluster of Au_2−Pt_2/TiO_2. The saturated adsorption amounts of RSSR on Au(TiO_2), Pt(TiO_2), and Au−Pt(TiO_2) were reasonably correlated to the adsorption energies obtained

from the DFT calculations for the corresponding model clusters. The present study has demonstrated that the core−shell type bimetallic cluster loaded TiO_2 exhibits a unique adsorption property that is different from those of the single metal systems, as a result of electronic modification of the shell metal through its interaction with the core metal and the support. The Au−Pt/TiO_2 photocatalytic reaction of the SCC is currently under investigation.

Acknowledgment. The authors express sincere gratitude to Ishihara Techno Co. for the gift of the TiO_2 particles (A-100).

References and Notes

(1) Bard, A. J. *Science* **1980**, *207*, 139.
(2) Linsebigier, A. L.; Lu, G.; Yates, J. T., Jr. *Chem. Rev*. **1995**, *95*, 735 and references therein.
(3) Wold, A. *Chem. Mater*. **1993**, *5*, 280.
(4) Tada, H.; Teranishi, K.; Inubushi, Y.-i.; Ito, S. *Chem. Commun*. **1998**, 23.
(5) Tada, H.; Teranishi, K.; Inubushi, Y.-i.; Ito, S. *Langmuir* **2000**, *16*, 3304.
(6) Sinfelt, J. H.; Via, G. H.; Lytle, F. W. *J. Chem. Phys*. **1980**, *72*, 4832.
(7) Nunez, G. M.; Rouco, A. J. *J. Catal*. **1988**, *111*, 41.
(8) Asakura, K.; Iwasawa, Y.; Yamada, M. *J. Chem. Soc., Faraday Trans. 1* **1988**, *84*, 2457.
(9) Baba, R.; Nakabayashi, S.; Fujishima, A.; Honda, K. *J. Am. Chem. Soc*. **1987**, *109*, 2273.
(10) Tada, H.; Teranishi, K.; Ito, S.; Kobayashi, H.; Kitagawa, S. *Langmuir* **2000**, *15*, 6077.
(11) Tsubota, S.; Haruta, M.; Kobayashi, T.; Ueda, A.; Nakahara, Y. In *Preparation of Catalysts V*; Poncelet, G., Jacobs, P. A., Grange, P., Delmon, B., Eds.; Elsevier: Amsterdam, 1991.
(12) Frisch, M. J.; Trucks, G. W.; Schlegel, H. B.; Scuseria, G. E.; Robb, M. A.; Cheeseman, J. R.; Zakrzewski, V. G.; Montgomery, J. A., Jr.; Stratmann, R. E.; Burant, J. C.; Dapprich, S.; Millam, J. M.; Daniels, A. D.; Kudin, K. N.; Strain, M. C.; Farkas, O.; Tomasi, J.; Barone, V.; Cossi, M.; Cammi, R.; Mennucci, B.; Pomelli, C.; Adamo, C.; Clifford, S.; Ochterski, J.; Petersson, G. A.; Ayala, P. Y.; Cui, Q.; Morokuma, K.; Malick, D. K.; Rabuck, A. D.; Raghavachari, K.; Foresman, J. B.; Cioslowski, J.; Ortiz, J. V.; Stefanov, B. B.; Liu, G.; Liashenko, A.; Piskorz, P.; Komaromi, I.; Gomperts, R.; Martin, R. L.; Fox, D. J.; Keith, T.; Al-Laham, M. A.; Peng, C. Y.; Nanayakkara, A.; Gonzalez, C.; Challacombe, M.; Gill, P. M. W.; Johnson, B. G.; Chen, W.; Wong, M. W.; Andres, J. L.; Head-Gordon, M.; Replogle, E. S.; Pople, J. A. *Gaussian 98*; Gaussian, Inc.: Pittsburgh, PA, 1998.
(13) Gill, P. M. W.; Johnson, B. G.; Pople, J. A. *Int. J. Quantum Chem. Symp.* **1992**, *26*, 319.
(14) Slater, J. C. *Phys. Rev*. **1951**, *81*, 385.
(15) Becke, A. D. *Phys. Rev*. **1988**, *A38*, 3098.
(16) Lee, C.; Yang, W.; Parr, R. G. *Phys. Rev*. **1988**, *B37*, 785.
(17) Vosko, S. H.; Wilk, L.; Nusair, M. *Can. J. Phys*. **1980**, *58*, 1200*l*; Wilk, L.; Vosko, S. H. *J. Phys. C: Solid State Phys*. **1982**, *15*, 2139.
(18) (a) Hay, P. J.; Wadt, W. R. *J. Chem. Phys*. **1985**, *82*, 270. (b) Wadt, W. R.; Hay, P. J. *J. Chem. Phys*. **1985**, *82*, 284. (c) Hay, P. J.; Wadt, W. R. *J. Chem. Phys*. **1985**, *82*, 299.
(19) Dunning, T. H., Jr.; Hay, P. J. In *Modern Theoretical Chemistry*; Schaefer, H. F., III, Ed.; Plenum Press: New York, 1976; 1.
(20) Tada, H.; Suzuki, F.; Yoneda, S.; Ito, S.; Kobayashi, H. *Phys. Chem. Chem. Phys*. **2001**, *3*, 1373.
(21) Lilie, V. J.; Beck, G.; Henglein, A. *Ber. Bunsen-Ges. Phys. Chem*. **1971**, *75*, 458.
(22) Fung, S. C. *J. Catal*. **1982**, *76*, 225.
(23) Tanaka, K.; Miyahara, K.; Toyoshima, I. *J. Phys. Chem*. **1984**, *88*, 3504.
(24) Tauster, S. J.; Fumg, S. C.; Baker, R. T. K.; Horsley, J. A. *Science* **1981**, *211*, 1121.
(25) Sato, S. *J. Catal.* **1985**, *92*, 11.
(26) Horsley, J. A. *J. Am. Chem. Soc*. **1979**, *101*, 2870.
(27) Brus, L. *J. Phys. Chem*. **1986**, *90*, 2555.
(28) Eastman, D. E. *Phys. Rev. B* **1970**, *2*, 1.
(29) Mulvaney, P.; Giersig, M.; Henglein, A. *J. Phys. Chem. B* **1992**, *96*, 10419.
(30) Huheey, J. E.; Keoter, E. A.; Keiter, R. L. *Inorganic Chemistry—Principles of Structure and Reactivity*, 4th ed.; Harper Collins College Pub.: New York, 1993; p 190.
(31) Stern, D. A.; Wellner, E.; Salaita, G. N.; Laguren-Davison, L.; Lu, F.; Batina, N.; Frank, D. G.; Zapien, D. C.; Walton, N.; Hubbard, A. T. *J. Am. Chem. Soc*. **1988**, *110*, 4885.
(32) Bryant, M. A.; Joa, S. L.; Pemberton, J. E. *Langmuir* **1992**, *8*, 753.
(33) Ulman, A. *Chem. Rev*. **1996**, *96*, 1553 and references therein.
(34) Gui, J. Y.; Lu, F.; Stern, D. A.; Hubbard, A. T. *J. Electroanal. Chem.* **1990**, *292*, 245.
(35) The number of atoms constituting a single Au particle (ca. 470 atoms) multiplied by the dispersion yielded the number of the surface Au atoms (ca. 120 atoms). For cubooctahedral packing, the dispersion is approximately 0.25 at $r \cong 1.5$ nm: G. A. Somorjai: *Introduction to Surface Chemistry and Catalysis*; John Wiley & Sons: New York 1994; p 10.
(36) Jennings, G. K.; Labinis, P. E. *J. Am. Chem. Soc*. **1997**, *119*, 5208.